NATIONAL ADVISORY COMMITTEE FOR AERONAUTICS

TECHNICAL MEMORANDUM

No. 1190

TESTS OF CASCADES OF AIRFOILS FOR RETARDED FLOW

By Yoshinori Shimoyama

Washington

October 1947

NATIONAL ADVISORY COMMITTEE FOR AERONAUTICS

TECHNICAL MEMORANDUM NO. 1190

TESTS OF CASCADES OF AIRFOILS FOR RETARDED FLOW[1]

By Yoshinori Shimoyama

Test results are present for cascades of airfoils in retarded flow
and increasing pressure as corresponds to the case of the impeller of an
axial propeller pump and propeller fan.

INTRODUCTION

Because of the varying distance between the blades of machines of
the axial flow type of propeller further progress in the design of these
machines on the basis of the so-called momentum theory is very difficult.
The author has already pointed out the difficulty in the design of such
machines by the momentum theory alone and has fully discussed the possi-
bility of resolving a great many of these difficulties by the application
of the recently developed airfoil theory (reference 1). However, in apply-
ing the airfoil theory to the impeller there is still one point that has
not been sufficiently clarified — namely, the problem of cascade interfer-
ence.

Since near the normal operating conditions the flow in all propeller-
type machines may be considered as axial, if the impeller is cut along
the cylindrical surface and developed, the problem can be reduced to that
of a plane cascade of airfoils. Figure 1 shows the developed cylinder
for a propeller pump or propeller blower, l being the airfoil chord, t
the spacing, θ the angle between the chord and the cascade direction.
The flow enters with velocity w_1 relative to the cascade, is deflected
by the airfoils and flows out with velocity w_2. From these the average
velocity w_∞ is obtained and the angle θ determined which corresponds
to the angle of attack α for the required lift with respect to w_∞.
The required lifting force is determined with reference to the difference
$w_{u1} - w_{u2}$ of the velocity components of the inlet and outlet velocities

w_1 and w_2 in the direction of the cascade axis and the gap-to-chord ratio t/l. A suitable airfoil is chosen and from the relation between the lift coefficient and angle of attack for the case of the isolated airfoil in two-dimensional flow the angle of attack α corresponding to the required lift can be determined.[1]

This method, which is based on the average velocity w_∞, takes into account the cascade effect to some extent and it thus becomes a question of applying the results to the isolated airfoil in two-dimensional flow. Recently this subject has received much theoretical investigation. Numachi (reference 3) and Weinig (reference 4) computed the ratio of the lift coefficients for the airfoil in cascade and when isolated for a cascade of plates and presented their results graphically. Schilhansl (reference 5) by an approximate method gave numerical results for the plate and circular arc airfoil. Detailed test results in this field are very meager. On impellers such as those of a propeller-type pump or fan where the pressure increases along the blades and the velocity decreases — denoted here as a retarded flow cascade — there are, besides the tests of Christiani (reference 6), only two or three other investigations. Since none of these are in sufficiently good agreement with theoretical results more detailed tests of wider scope are necessary.

The author has undertaken tests to investigate the interference effect of retarded flow airfoil cascades within the scope of the usual propeller pump and propeller fan, and the results of the completed tests are here presented.

TEST APPARATUS AND PROCEDURE

A newly constructed 50-centimeter-square tunnel was especially used for this purpose (reference 7). The tunnel had a 53-centimeter-square exit cone. The flow past the cascade mounted in the exit cone was deflected during the tests. Since this deflection varied with the angle between the airfoil setting and the inlet flow direction, the flow past the cascade, was discharge in the atmosphere to avoid turbulence. The velocity in the bell differed from that at the center by an average of +0.4 and -0.2 percent. The static pressure was practically uniform along the entire section and there was no rotational component of the velocity. The airspeed was generally 30 meter per second, varying somewhat with the incidence of the cascade.

---

[1]In obtaining w_∞ the lift coefficient, etc. the velocity component with respect to the drag in the cascade axis direction must also be considered. On this, see reference 2.

The airfoil section used in the test approximated the Göttingen airfoil No. 549; the chord was 10 centimeters, and the span of 53 centimeters was equal to the length of a side of the bell. By applying end plates at the tips the flow obtained was made to approach the two-dimensional. Since the ideal case of an infinite number of airfoil blades cannot, of course, actually be realized, the tests generally were conducted with five blades and, in some cases, seven and nine the results for which are a good approximation of the ideal case of an infinite number of blades. Since the pressure differed at the inlet and outlet sides of the cascade, top and bottom plates were placed on the upstream side. Figures 2 and 3 show these arrangements.

The force acting on an airfoil of the cascade was obtained by measuring the pressure distribution over the middle section of the center airfoil. For this purpose the center airfoil alone was specially made of brass (the others were all made of wood) and 20 small orifices of 0.25 centimeter diameter were arranged over the middle section of this airfoil as indicated in figure 4 and tubes inserted into the airfoil led to a multiple-tube manometer.

The multiple-tube manometer used alcohol. The tube diameters were sufficiently large and uniform so as to avoid capillarity error as far as possible. The glass tubes of the manometer each received careful inspection. The pressure indicated by this manometer over the airfoil section, the dynamic pressure at the inlet, the static pressure, and other required recordings were simultaneously photographed, and the readings were all obtained from the dry plates. Figure 5 shows an example of such a photograph. With the aid of the light reflected from the surface of the liquid in the tubes a good photograph could be obtained.

The angle β_1 between the cascade-axis direction and the inlet-flow direction was determined by the oblique angle cut off by the end plates at the two sides of the exit cone. Each of the airfoils of the cascade was freely rotatable. Since the direction of the chord could be read on a scale as shown in figure 6, the angle α_1 between the inlet velocity and the chord could be regulated as desired. The angle θ between the cascade axis and the chord as shown in figure 2 is readily obtained from

$$\theta = \beta_1 + \alpha_1 \qquad\qquad (1)$$

The static pressure at the inlet and the velocity of the stream were measured with the aid of an NPL type pitot tube located at a (fig. 2). Since the location of the pitot tube was at some distance from the center airfoil, the losses occurring in between and the non-uniformity of the velocity, which, however, is slight, must be taken into account. For this purpose a small static pressure orifice was placed as

near as possible to the cascade b, (fig. 2) and the pressure drop be-
tween the pitot tube and this orifice was measured for varying α_1.
Since the losses from b to the center airfoil cannot be measured in the
presence of the cascade, the difference in pressure between b and c
with the airfoils removed is measured and the pressure drop due to the
losses from the pitot tube location a to the center airfoil can be
obtained. Moreover, if the difference between the total pressure measured
by the pitot tube and the total pressure at the leading edge of the center
airfoil is obtained and this value is exactly equal to the losses incurred
on the way, the flow velocity at the pitot tube and that at the center air-
foil are equal. If this difference is smaller (or greater) than the losses
incurred on the way, the flow velocity at the center airfoil is greater
(or smaller) than the flow velocity at the pitot tube. Thus it is possible
by the pitot tube measurements alone to determine the corrections on the
velocity.

In the tests β_1 and t (or t/l) were held constant and α_1
varied, the multiple-tube manometer was photographed each time and the
pressure distribution and other required readings simultaneously recorded.
An example of such a photograph (fig. 5) has already been mentioned.

The value of θ for a propeller pump or propeller fan usually lies
between 10° and 30° and t/l between 1 or 2, rather large values being
used for the fan. If t/l is large, however, the interference effect
due to the neighboring airfoils becomes smaller and the tests were there-
fore conducted for the following range of values: $t/l = 0.75$, 1, 1.5, 2,
$\beta_1 = 10^{\circ}$, 12.5°, 15°, 17.5°, 20°, 22.5°, 25°. For these 28 combinations
seven values of α_1 were used — namely, $\alpha_1 = -5^{\circ}$, -2.5°, 0°, 2.5°, 7.5°,
10°. With t/l and θ as parameters α as the variable the lift and
drag coefficients were varied with α and the effect of t/l and θ on
the change in lift and drag coefficients as compared with the isolated air-
foil thus could be determined.

<center>PRESENTATION OF THE RESULTS AND PRESSURE DISTRIBUTION</center>

The pressure distribution was first measured over the single airfoil,
of the same section as that of the airfoils cascade in two-dimensional
flow obtained with the side plates. The pressures were all expressed as
fractions of the dynamic pressure and plotted with the chord and the
perpendicular to it as coordinate axes. An example is shown in figure 7.
Calling X and Y the forces acting on unit width along and perpendicular
to the chord, respectively, results in

$$C_x \gamma l \frac{w^2}{2g}, \quad Y = C_y \gamma l \frac{w^2}{2g} \qquad (2)$$

The coefficients C_y and C_x can be obtained by measuring the areas of the left and right sides, respectively, of figure 7. In the foregoing equations γ is the density of the fluid, l is the length of the chord, w the velocity of the fluid, and g the acceleration of gravity. Furthermore, since the angle α between the wind direction and the chord is known, the single airfoil lift coefficient Cae and drag coefficient Cwe can be immediately obtained from the following equations

$$Cae = C_y \cos\alpha - C_x \sin\alpha$$
$$Cwe = C_x \cos\alpha + C_y \sin\alpha$$

(3)

Since the foregoing drag coefficient is obtained from the pressure distribution it is smaller than the experimental drag coefficient by the amount of the surface friction, but for convenience will still be denoted simply as the drag coefficient.

The lift and drag coefficients were obtained from the pressure distributions, although this involved considerable difficulty. This was unavoidable, however, because the wind tunnel was not provided with a balance.

As in the case of the single airfoil the pressures over the airfoils in cascade were expressed in fractions of the dynamic pressure at the inlet and plotted with the chord and the perpendicular to it as coordinate axes. Figures 8 to 10 show several of these obtained diagrams. The static pressure at the inlet was used as a standard for the pressures over the airfoils.

Figure 8, with β_1 and α_1 and therefore according to (1) also θ fixed, shows the effect of t/l on the pressure distribution. It is seen that if t/l is small the pressure variation is rather steep, particularly for the case of $t/l = 0.75$ in which the trailing edge of the airfoil approaches the leading edge of the airfoil on the right, (fig. 1), the negative pressure is greatly increased. Again, in the neighborhood of the leading edge as the latter approaches the trailing edge of the airfoil on the left there is a notable increase in the negative pressure. As is seen by comparing figure 30 with figure 8, this effect is increased if θ is small, since the airfoils then approach each other even more closely. In the case in which t/l is small, the considerable negative pressure arising at the leading edge helps to explain the cavitation phenomenon near the leading edge at the pressure side of a marine propeller and at the inlet of the spiral casing of a pump.

Figure 9 shows the pressure distribution with varying β_1 and therefore θ for fixed values of t/l and α. As may be seen from this figure, if α_1 is not too large, the pressure distribution and therefore the lift coefficient is not greatly affected by θ.

Figure 10 shows the change in pressure distribution with α_1 for fixed values of t/l and β_1. A comparison with the case of the single airfoil (fig. 7) is of considerable interest.

The determination of the velocity components perpendicular and parallel, respectively, to the direction of the inlet velocity w_1 from the pressure distribution is the same as for the single airfoil. Since, in this case, the inlet velocity w_1 is used instead of w, the coefficients are all denoted with a subscript 1, and equation (2) becomes

$$X = C_{x1}\gamma l \frac{w_1^2}{2g} \qquad Y = C_{y1}\gamma l \frac{w_1^2}{2g} \qquad (2a)$$

The coefficients C_{x1} and C_{y1} are determined by graphical integration, as in the case of the single airfoil. The force components referred to unit width of airfoil at right angles and parallel, respectively, to the direction of w_1 are

$$A_1 = C_{a1}\gamma l \frac{w_1^2}{2g} \qquad W_1 = C_{w1}\gamma l \frac{w_1^2}{2g} \qquad (4)$$

where C_{a1} and C_{w1}, similar to the case of equation (3), can be obtained from

$$\left. \begin{array}{l} C_{a1} = C_{y1}\cos\alpha_1 - C_{x1}\sin\alpha_1 \\ C_{w1} = C_{x1}\cos\alpha_1 + C_{y1}\sin\alpha_1 \end{array} \right\} \qquad (3a)$$

As in the case of the airfoil cascade, the lift coefficient is taken with respect to the average of the inlet and outlet velocities w_∞ (fig. 1). The force components, referred to unit width of the airfoil at right angles and parallel, respectively, to the direction of w_∞ are

$$A = C_a\gamma l \frac{w_\infty^2}{2g} \qquad W = C_w\gamma l \frac{w_\infty^2}{2g} \qquad (5)$$

from which C_a and C_w are obtained. Putting $\beta - \beta_1 = \delta$ gives

$$A = A_1\cos\delta + W_1\sin\delta$$

and substituting relations (4) and (5) in the foregoing equation results in

$$\frac{C_a}{C_{a1}} = \left(\frac{w_1}{w_\infty}\right)^2 \left(\cos\delta + \frac{C_{w1}}{C_{a1}}\sin\delta\right)$$

Within the range of the tests conducted large values of δ did not frequently; the value of the ratio C_{w1}/C_{a1} was likewise small. More-over, even in the case in which C_{a1} is very small, the value of $\sin\delta/C_{a1}$ from equation (10) and others is considerably less than 1. Hence, without too great error it is possible to put

$$\frac{C_a}{C_{a1}} \approx \left(\frac{w_1}{w}\right)^2 \tag{6}$$

If δ is small it is possible to

$$w_1 \approx w_\infty + \frac{w_{u1} - w_{u2}}{2}\cos\beta_1$$

But

$$w_{u1} - w_{u2} = \frac{\Gamma}{t} = \frac{C_a l w_\infty}{2t}$$

hence

$$w_1 = w_\infty + \frac{C_a l w_\infty}{4t}\cos\beta_1 \tag{7}$$

where $\Gamma = \frac{1}{2} C_a l w_\infty$ is the circulation around the wing. Next, by substituting equation (7) in (6) and rearranging, there is obtained

$$\frac{1}{16} C_{a1}^2 \left(\frac{l}{t}\right)^2 \cos^2\beta_1 \left(\frac{C_a}{C_{a1}}\right)^2 - \left(1 - \frac{1}{2} C_{a1}\frac{l}{t}\cos\beta_1\right)\frac{C_a}{C_{a1}} + 1 = 0$$

a second-degree equation in C_a/C_{a1}. By setting

$$C_{a1}\frac{l}{t}\cos\beta_1 = x \tag{8}$$

and solving the equation (8) for C_a/C_{a1}, there is obtained

$$\frac{C_a}{C_{a1}} = \frac{4(2 - x - 2\sqrt{1 - x})}{x^2} \tag{9}$$

where the $\pm$ sign before the square root was chosen from the consideration that $C_a/C_{a1} = 1$ for $t/l = \infty$ — that is, $x = 0$. Having obtained C_{a1}, x is obtained from equation (8) and C_a can then be obtained from equation (9).

If δ is small, it can be obtained from

$$\delta \approx \frac{w_{u1} - w_{u2}}{2w_\infty} \sin\beta_1 = \frac{C_a l}{2t} \sin\beta_1 \quad \text{rad}$$

$$= 14.3 \frac{l}{t} C_a \sin\beta_1 \tag{10}$$

and the angle of attack α can then be obtained from

$$\alpha = \alpha_1 - \delta \tag{11}$$

Again, since

$$W = W_1 \cos\delta - A_1 \sin\delta$$

from (4), (5), and (6)

$$C_W = (C_{W1} \cos\delta - C_{a1} \sin\delta) \frac{C_a}{C_{a1}} \tag{12}$$

from which C_W can be obtained.

TEST RESULTS

The lift and drag coefficients C_{ae} and C_{we} for the case of the single airfoil were obtained from the pressure distribution by graphical integration, and the results are shown in figure 11. Figures 12 to 15 show the lift coefficient for the airfoil in cascade. In each case the

number of airfoils used was five. The lift coefficient was obtained from the pressure distribution over the middle section of the center airfoil and, as in figure 11, C_a was plotted against the angle of attack α. In order to show the measured points more clearly on these figures, the ordinate axis was shifted for the various values of θ. Figures 16 to 19 show the curves for the original points.

Figure 16 gives the results for $t/l = 2$. For small values of the lift coefficients, the curves practically merge into one. It is seen that the effect of θ for the range $12.5° \leqq \theta \leqq 25°$ is not large, but as θ increases, the maximum value attained by the lift coefficient tends to increase. In any case, however, the maximum lift coefficient attained is only a little smaller than that for the single airfoil. The angle of attack for zero lift does not agree with the corresponding angle for the single airfoil but is shifted toward a greater value. The slope of the curve of lift against angle of attack is greater than the slope for the single airfoil case. Hence, in spite of the shift of the zero - lift angle to the right for large values of the lift coefficient, cases arise where the latter is equal to or greater than the lift coefficient for the single airfoil.

Figure 17 shows the case for $t/l = 1.5$. The curves show the same tendency as for $t/l = 2$, but since the airfoils are now closer, the interference effect is greater than in the preceding case. The slope of the lift curve is steeper, the maximum lift coefficients are smaller, and the zero-lift angle of attack is greater.

Figure 18 shows the case for $t/l = 1$. The slopes of the lift curves are still greater, the maximum lift coefficients smaller, and the zero-lift angle of attack greater. For $t/l = 2$ and $t/l = 1.5$ the zero-lift angle of attack is practically constant for any value of θ within the range $12.5° \leqq \theta \leqq 25°$, but for $t/l = 1$ the effect of θ is evident, becoming more marked with decreasing θ. Although the slope of the lift-coefficient curves is steep for small values of the lift coefficient, and the zero-lift angle of attack is large as compared with that of the single airfoil, the curves do not intersect the curve for the single airfoil in the range $12.5° \leqq \theta \leqq 25°$. Hence the ratio C_a/C_{ae} for this case is always less than 1.

Figure 19 shows the results for $t/l = 0.75$. Since in this case the airfoils are much closer together, the curves show a different character than for the previous three cases. Especially for small values of θ since the airfoils approach each other still more, the different tendency is marked. For small values of the lift coefficient the curves resemble those for $t/l = 1$.

From the foregoing results it is seen that with decreasing t/l the zero-lift angle of attack is shifted toward greater values. Furthermore, the effect of θ is evident for small values of t/l - namely, 1 and 0.75. To show clearly the variation of the amount of this shift, the difference between the zero-lift angles for the cascade and the single airfoil was plotted against t/l, as shown in figure 20. The following consideration may be given as the reason for this shift in the angle of attack for zero lift. In using an airfoil section of thickness and camber such as are met in an airplane wing in a retarded flow cascade, the effect of the neighboring airfoil is obtained as t/l becomes smaller (in fig. 1 the effect of the flow along the back of the neighboring airfoil to the left). Actually the direction of the flow at the inlet differs by a small angle from the direction of the flow at a great distance. This effect is more marked as t/l becomes smaller and increases with smaller θ. This is clearly in good agreement with the test results, as is seen in figure 20. This also explains the large negative pressure near the heading edge of the surface.

It is generally assumed that for small t/l the direction of the flow at the outlet agrees with the direction of the tangent at the outlet edge. This is in complete agreement with the results obtained by Weinig (reference 4) on the flat-plate cascade for $t/l < 0.7$. If this assumption were also true for a cascade of airfoils having thickness and camber for small t/l and the outlet flow where in the direction of the tangent to the outlet edge, the changes in the inlet and outlet directions would be very small and the lift therefore would be zero. Hence the zero-lift angle of attack, as t/l gradually becomes smaller, must agree with the direction of the outlet edge. For the cascades of airfoils used in these tests the direction of the outlet edge corresponded to an angle of attack of about -8.8°, but as t/l became smaller the zero-lift angle of attack had no tendency to approach -8.8°. On the contrary, as shown clearly in figures 15 to 20, it moved in the opposite direction. This can be understood by consideration of figure 21, showing a retarded flow cascade of airfoils for the case where t/l and θ are both small. Although t/l is small, the effect of thickness and camber is such that the outlet-flow direction does not necessarily agree with the direction of the outlet edges.

The zero-lift angle of attack for the retarded flow cascade of airfoils is considerably greater than the angle corresponding to the single airfoil, and in finding the interference coefficient or the ratio C_a/C_{ae} an important relation is obtained. If this ratio following general practice (reference 8) is taken for the same angle of attack, the interference coefficient even for t/l and θ fixed varies greatly with the angle of attack and is certainly not constant. The point will be discussed below.

It should be observed that a far smaller value for the maximum lift coefficient for a retarded flow cascade was obtained than for the single airfoil. If only the test results for the single airfoil are considered and the impeller designed by using the value of the lift coefficient on the assumption that it is sufficiently accurate, the expected lift coefficient will be greater than the maximum lift coefficient corresponding to the values of t/l and θ for the impeller under consideration since according to the test results given the case of small t/l must be considered. C. Keller (reference 9), using the value $t/l = 1.39$ for the blade tip of the impeller and $t/l = 0.97$ near the middle and the respective values $C_a = 0.845$ and 1.0 in computing a fan with small t/l, obtained results entirely at variance with test results. The reason is to be found in the considerations discussed.

The outlet velocity of a retarded-flow cascade is smaller than the inlet velocity and, since this gives rise to a difference in pressure, the flow along the trailing edge of the airfoil is more strongly retarded as compared with that of a single airfoil. Since the flow is in the direction of increasing pressure, separation must also occur earlier than for the single airfoil. This explains why the maximum lift coefficient for the retarded flow cascade is considerably less than that for the single airfoil.

The drag coefficients are given in figures 22 to 25. All values were obtained from the pressure distribution over the center section of the center airfoil of a 5-blade cascade and, to bring out the test points clearly, the abscissa axis was displaced for each different value of θ. For convenience in comparison, the original points are given in figures 26 to 29. For comparison, the drag coefficient for the single airfoil is given by the dotted curves marked $t/l = \infty$. In all cases, the drag coefficient for the cascade is greater than for the single airfoil. Its smallest value for $t/l = 2$ and $t/l = 1.5$, for which the spacing is somewhat greater than the smallest value for the single airfoil, and the difference increases for $t/l = 1$ and 0.75 as the spacing becomes smaller. Furthermore, for small angle of attack (negative value) C_w increases with decreasing t/l. For large angle of attack C_w increases decreasing θ. For large angle of attack C_w is greater for $t/l = 1.5$ than for $t/l = 2$. As the spacing becomes closer, the effect of θ becomes more marked. For small θ and increasing angle of attack, C_w rapidly increases, but for large θ the rate of increase is smaller. For $t/l = 1$ and 0.75 and large θ C_w is smaller than for $t/l = 1.5$ for large angles of attack.

As t/l becomes less than 1 and the blades approach each other the drag coefficient increases. As may be seen from the pressure distribution curve of figure 8 for the case of $t/l = 0.75$ as the pressure is gradually recovered on the back of the wing the latter receives the effect of the

neighboring wing resulting in a lowered pressure, increased resistanve of the back side, and hence increaeed drng coefficient. The drag coefficient for the case of $t/l = 0.75$ is particularly affected by the value of θ. When θ is small, since the airfoils are then closer together, the increas mentioned in the resistance of the back of the wing becomes more marked. This becomes clearer when figure 8 for $t/l = 0.75$ is compared with figure 30. However, even for $t/l = 0.75$ if θ is large and the distance between the airfoils relatively greater, there is practically no increase in the resistance on the back of the airfoil and even for large angles of attack the drag does not become so large. If the passage around each blade is considered for $t/L = 0.75$, it will be seen that for the thickness of section used the conditions will be more favorable for larger θ than for small θ, so that the losses are smaller and hence the drag is smaller.

For the normal operating conditions it is desirable so to determine the blade setting that the value of the ratio of the drag[1] to lift coefficients $\epsilon = C_w/C_a$ is the least possible. According to these considerations the angle of attack corresponding to the smallest ϵ varies with t/l and θ and differs frcm the angle of attack corresponding the least value of ϵ for the single airfoil.

The above results were all for a five-blade cascade. Practically all similar tests have been conducted for five blades on the supposition that the results for an infinite number of blades are thereby approached. The author, with the object of clarifying this point carried out tests with seven blades and nine blades for $t/l = 1$ and with seven blades for $t/l = 1.5$. In each case the lift and drag coefficients were obtained from the pressure distributions at the center section of the center airfoil exactly as for the case of five blades.

Figures 31 to 32 show the results for seven and nine blades, respectively, for the case $t/l = 1$. In each case the axis of ordinates was displaced in the same manner as for figure 14. Figures 33 and 34 show the same curves not displaced. For comparison, the dotted curves for the single airfoils indicated by $t/l = \infty$. Comparison of these figures with figure 18 shows that the lift curves greatly resemble each other. For small lift coefficient the slope is not much affected by the number of blades. As the number of blades increases, the whole family of curves is shifted to the right. This shift is shown most clearly by plotting the change in the zero-lift angle of attack. In figure 35 the difference between the zero-lift angle of attack for the single airfoil and cascade is plotted as the ordinate against the number of blades as the abscissa.

---

[1]The drag here considered was obtained from the pressure distribution and the drag due to skin friction must be added to obtain the true drag coefficient.

As may be seen from the figure for $t/l = 1$ there is some shift in the lift curve for five and seven blades and a smaller shift for seven and nine blades; whereas the results obtained for nine blades are seen to approach the case of an infinite number of blades. The maximum lift coefficient decreases with the increasing number of blades, as the difference for seven to nine blades is less than that for five to seven blades. To bring out these results more clearly, the lift curves for five, seven, and nine blades and for the single blade for the case in which $\theta = 20°$ are shown in figure 36.

Figure 37 shows the results for seven blades for $t/l = 1.5$. The number of test points is unfortunately small, but by referring to the results for $t/l = 1.5$ and five blades and $t/l = 1$ with a greater number of blades the curves of figure 37 could easily be constructed. Compared with figure 17, the curves of lift coefficient against angle of attack are shifted somewhat to the right. The increase in the zero-lift angle of attack above that for the single airfoil is shown by the dotted curve in figure 35. The shift in the lift curve when the number of blades increases from five to seven is seen to be much less for $t/l = 1.5$ than for $t/l = 1$. The maximum lift coefficient for seven blades is smaller than that for five blades. These relations can also be seen from the example shown in figure 38.

The drag coefficient for $t/l = 1$ and $t/l = 1.t$ is not appreciably affected by the number of blades, approximately the same values being obtained as for the case of five blades.

Since the number of blades of an impeller of any installation can-not be conveniently increased and tests conducted, it is considered that the preceding test results provide information as to the results for an infinite number of blades.

DISCUSSION OF RESULTS

For the flat-plate cascade the theoretical value of C_a/C_{ae} has been given by Numachi (reference 3), Weinig (reference 4), and Schilhansl (reference 5) as a function of t/l and θ. The following figures and table are taken from the papers of these authors.

Weinig obtained the interference coefficient from the isocline trans-formation, and his results are in good agreement with the values obtained by an approximate method by Schilhansl. This interference coefficient for the flat-plate cascade has a fixed value for fixed t/l and θ irrespective of the angle of attack. It is generally assumed that these approximate results hold true also for cascades of airfoils having thick-ness and camber. For an airfoil cascade with thickness and camber the question is what setting to choose so that it is equivalent to the θ of

the flat-plate cascade. Since for a flat-plate cascade, if the inlet flow
is in the direction of the plates, that is, zero angle of attack, there
is no lift, it would seem logical for the case of a cascade of airfoils
with thickness and camber to take the angle between the inlet flow and
the cascade direction for zero lift as the equivalent θ of the flat-plate
cascade. This direction is not, however, a characteristic direction of
airfoil and, as clearly shown by the author's tests, is affected by t/l
and θ. Although some difference arises between the value of θ as
determined from the angle between the zero-lift direction and the cascade
axis on the one hand and between the chord and the cascade axis on the
other, at any rate within the scope of these tests, the theoretical value
of C_a/C_{ae} must necessarily be greater than 1 and particularly for
$t/l = 1$ and small θ it must be rather large. On comparing figures
16 to 19 with table 1, however, it is clear that the test results are not
in entire agreement with the theory. Thus the flat-plate-cascade theory
is not entirely applicable directly to a retarded-flow cascade of airfoils
having finite thickness and camber.

Where is table 1 ?

    In figures 12 to 19 the dotted curves show the theoretical lift
curves as obtained from the results of Weinig for C_a/C_{ae} as a function
of t/l and θ_0, where θ_0 denotes the angle between the zero-lift
direction and the cascade axis. The curves were shifted to the right so
as to start from the point of zero lift. As may be seen from the curves
if this parallel shift is allowed for, the test results are in general
agreement with the theoretical. Closer consideration shows, however,
that for small experimental lift coefficient and fixed t/l the slope
of the lift curves is not greatly affected by the value of θ_0, the
slope becoming somewhat larger when θ_0 is large. As seen from table 1
the theoretical C_a/C_{ae} becomes smaller for the flat-plate cascade as
θ_0 becomes larger. Thus the best agreement of the theoretical results
with the author's tests for any value of t/l is generally for a value of
θ between the chord and the cascade axis in the neighborhood of $15°$. In
other words, the theoretical and experimental values for the range
$0.75 \lessapprox t/l \lessapprox 2$ are in approximate agreement in the neighborhood of
$\theta = 15°$. This is of great advantage in carrying over the test results
for a single airfoil to a cascade of airfoils.

    Figure 39 shows a representative example of the results of Christiani
on retarded flow cascades (reference 6). For comparison, there is also
given the lift-coefficient curve (shown dotted) obtained by the same
author for the single airfoil of section Göttingen No. 430. The curve,
corrected for two-dimensional flow was taken from the Göttingen report
(reference 10). The results have all been obtained for five blades.
Since each curve was drawn for fixed t/l and β_1 but with varying α_1
and hence varying θ no direct comparison could be made, but it is seen

in general that the results tend to agree with those of the author. The curve for $t/l = 1.07$, $\beta_1 = 33°41'$ differs from that for $t/l = 1.16$, $\beta_1 = 59°03'$ which is in close agreement with the curve for the single airfoil although t/l is approximately 1. But since β_1 in the latter case was outside the range of the author's tests, no comparison can be made.

Figure 40 shows the test results of Keller (reference 9) on a five-blade cascade for $t/l = 1.19$ and $\beta_1 = 23°20'$. The shift of the cascade to the right of the curve for the single airfoil (though the amount of the shift is somewhat smaller than that obtained by the present author) and the smaller maximum lift coefficient are in entire agreement with our test results. The test results of Ober obtained at the Massachusetts Institute of Technology on a five-blade cascade of symmetric section (Göttingen No. 429) were briefly described by Marks (reference 11). Although these results were not too accurate, they tend to agree general with those of the author.

In the tests of O'Brien (reference 12) on a propeller pump for a spacing $t/l = 1.7$ the lift coefficient for the single airfoil was used and the computed results on the volume flow of water were reported to agree approximately with the test results. Keller (reference 9) measured the velocity at the inlet and the outlet of an axial-flow fan and obtained the lift and drag coefficients for the operating conditions. By making use of those results and eliminating the effect of the rotational velocity component due to the drag, the lift coefficient was obtained as shown in figure 41. For comparison there is also given the lift coefficient for the single airfoil taken from the Göttingen report (reference 13). As may be seen from the figure, for the case of $t/l = 1.33$ C_a is somewhat smaller, but for $t/l = 1.76$ to 3.20 there is general agreement with the single airfoil.

In plotting the pressure of a propeller fan against the volume flow, a discontinuity is often obtained when the flow is small. According to the tests of Marks (reference 11) since the angle of attack at any section of the airfoil is smaller than the angle of attack of the single airfoil at which burbling arises, this phenomenon cannot be explained by burbling. According to the present author's tests flow breakdown arises relatively earlier in a retarded-flow cascade as compared with the single airfoil and since the phenomenon is also accompanied by noise, it is believed that it can be explained satisfactorily by burbling.

CONCLUSIONS

Tests were conducted in a wind tunnel of square exit cone 53 centimeters on a side. The tests generally were conducted for cascades of five airfoils, but some tests were conducted with seven and nine airfoils. From the pressure distribution over the center section the lift and drag coefficients (the drag coefficients due to the pressure distribution) only were obtained. By comparing these with the values obtained for the single airfoil, various interesting results were obtained.

The tests were conducted for the ranges $0.75 \lessgtr t/l \lessgtr 2$, $10^\circ \lessgtr \theta \lessgtr 30^\circ$, and the general results obtained were as follows:

1. At the pressure side of the airfoil there is a negative pressure region, and the negative pressure increases as t/l becomes smaller. For $t/l = 0.75$ when the blades are close to each other low pressure will also occur at the part of the airfoil where the leading edge of the following one is nearest to it. In both regions the negative pressure increases as θ becomes smaller.

2. The lift-coefficient curve is shifted to the right as compared with the curve for the single airfoil. The angle corresponding to zero lift therefore is greater than for the single airfoil, the amount of the increase becoming larger as t/l becomes smaller; moreover, for small t/l there is also the effect of θ.

3. The slope of the lift-coefficient curve for small values of the lift coefficient becomes larger with decreasing t/l, whereas θ appears to have little effect on the slope.

4. The maximum-lift coefficient of the retarded-flow cascade of airfoils is smaller than for the single airfoil and decreases with t/l. For this reason, in designing a propeller pump or fan impeller the results from tests on single airfoils cannot be applied directly.

5. The theory of the flat-plate cascade cannot be applied directly to a cascade of airfoils having thickness and camber.

6. The slope of the lift-coefficient curves agrees fairly well with the theoretical value for the flat-plate cascade, the agreement being quite good in the neighborhood of $\theta = 15^\circ$, but not so good for other values of θ. The agreement is also not very good when t/l is small.

7. The test results of Keller, Marks, and others on propeller pumps and fans agree with the results of the present tests.

8. The drag coefficient for the retarded-flow cascade is greater than that for the single airfoil and increases with decreasing t/l. For a large angle of attack the drag coefficient decreases as θ increases, and particularly when t/l is small the effect of θ is large.

9. The results obtained on the nine-airfoil cascade for $t/l = 1$ and on the seven-airfoil cascade for $t/l = 1.5$ may be considered to approach the results for an infinite number of blades. The lift curves for the seven- and nine-airfoil cascades for fixed t/l and θ closely resemble the curves for the five-blade cascade. The drag coefficient is not greatly affected by the increase in the number of airfoils, as the result was approximately the same for the five-blade cascade.

Translation by S. Reiss,
National Advisory Committee
for Aeronautics.

<div align="center">REFERENCES</div>

1. Shimoyama, Yoshinori: The Design of Axial Blowers. Jour. of Mech.
    Engrs., Kyushu Imperial Univ. (Japan), No. 40, 1937.

2. Shimoyama, Yoshinori: Contribution to the Design of Axial-Flow Propeller-
    Type Machines with their Housing. Kyushu Imperial Univ., Bul. 8, 2,
    1936.

3. Numachi, F.: Aerofoil Theory of Propeller Turbines and Propeller Pumps
    with Special Reference to the Effects of the Lifts and the Cavita-
    tion. Jour. Mech. Engrs., 1928, 31, 136.

4. Weinig, F.: Die Strömung um die Schaufeln von Turbomaschinen.
    Beitrag zur Theorie Axial Durchströmter Turbomaschinen, (1935).

5. Schilhansl, M.: Näherungsweise Berechnung von Auftrieb und Druck-
    verteilung in Flügelgittern. Jahrb. d. Wissensch. Gesellschaft für
    Luftfahrt (1927).

6. Christiani, K.: Experimentelle Untersuchung eines Tragflügel profils
    bei Gitteranordnung. Luftfahrtforschung, vol. 2, no. 4, Aug. 27,
    1928, pp. 91-110.

7. Shimoyama, Yoshinori: On the 59 cm Square Wind Tunnel. Kyushu
    Imperial Univ. Rep. 10, 4, 1935.

8. Pfleiderer: Die Kreiselpumpen. (2d ed.) 1932, pp. 115–121.

9. Keller, C.: Axialgebläse vom Standpunkt der Tragflügel Theorie
   (1934).

10. Wieselsberger, C., Betz, A., and Prandtl, L.; Ergebnisse der
    Aerodynamischen Versuchsanstalt zu Göttingen. I. Lieferung.
    R. Oldenbourg (Munchen and Berlin). (Christiani on Göttingen
    430 Airfoil.)

11. Marks, L. S., and Flint, T.: The Design and Performance of a High–
    Pressure Axial–Flow Fan. A.S.M.E. Trans., 57, 1935.

12. O.'Brien, M. P., and Folsom, R. G.: Propeller Pumps. A.S.M.E. Trans.,
    57, 1935.

13. Prandtl, L., and Betz, A.: Ergebnisse der Aerodynamischen Versuch–
    sanstalt zu Göttingen. II. Lieferung. R. Oldenbourg, 1927.
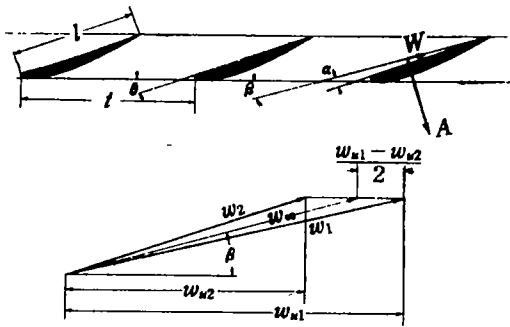
Figure 1.
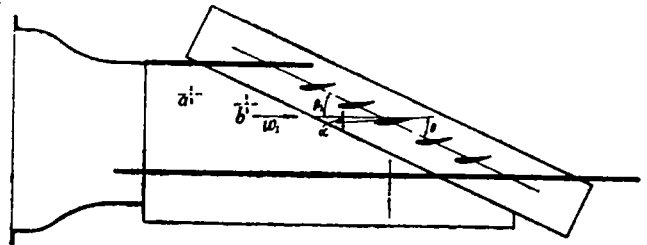
Figure 2.
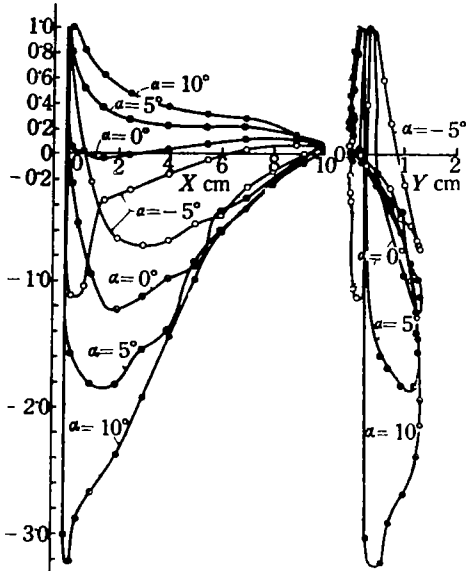
Figure 7.— Pressure distribution
for the single airfoil.
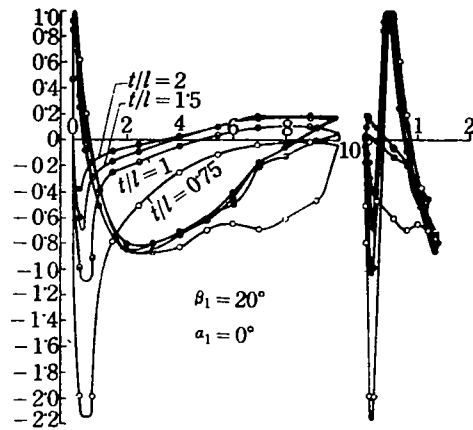
Figure 8.— Effect of t/l on the
pressure distribution.
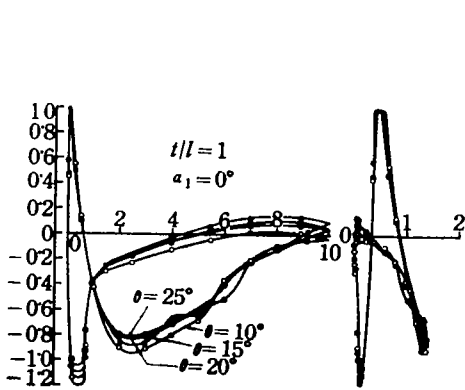
Figure 9.— Effect of θ on
the pressure
distribution.
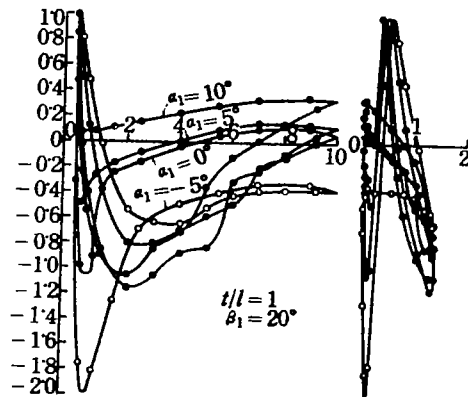
Figure 10.— Effect of α_1 on
the pressure
distribution.

Page intentionally left blank
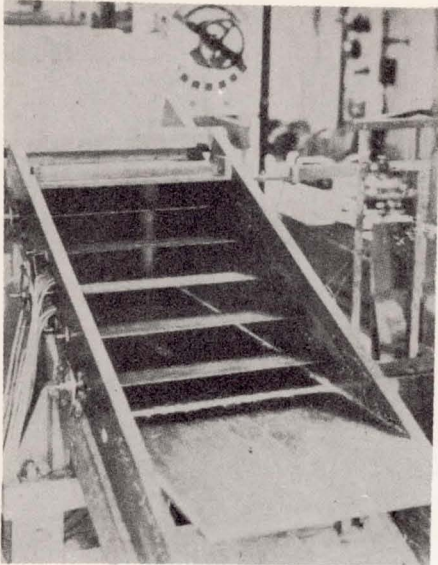
Figure 3.

Figure 4.- Arrangement of the
pressure orifices.
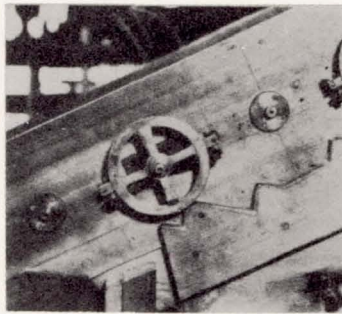
Figure 6.
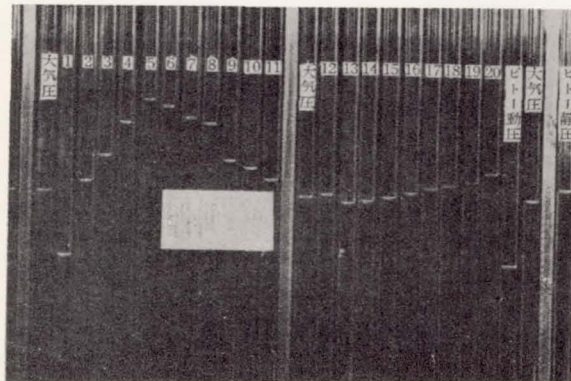
Figure 5.

Page intentionally left blank
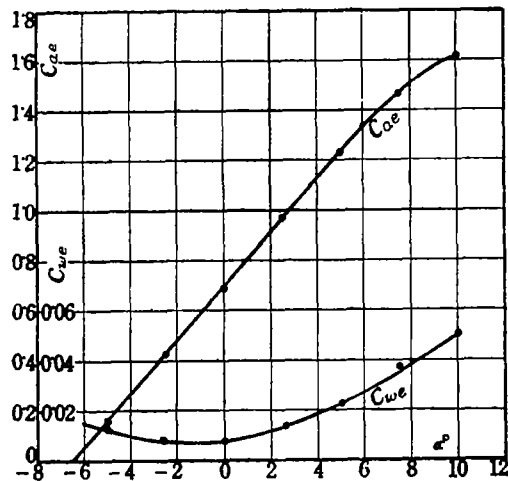
Figure 11.— Lift and drag coefficients for the single airfoil.
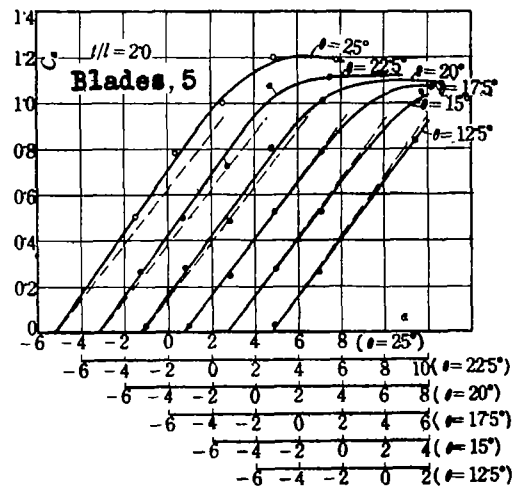
Figure 12.
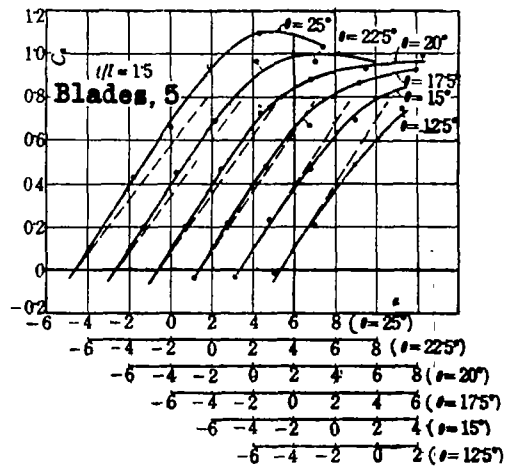
Figure 13.
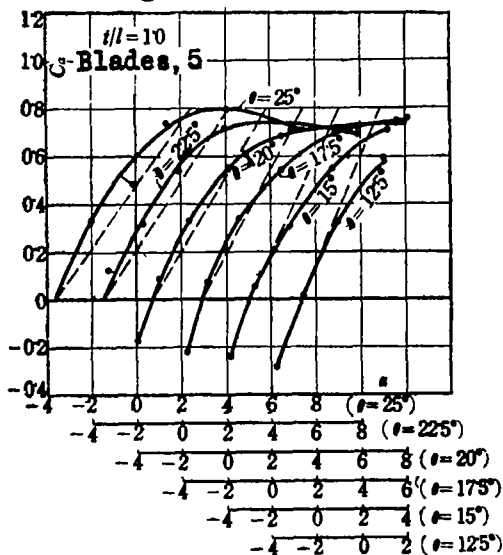
Figure 14.
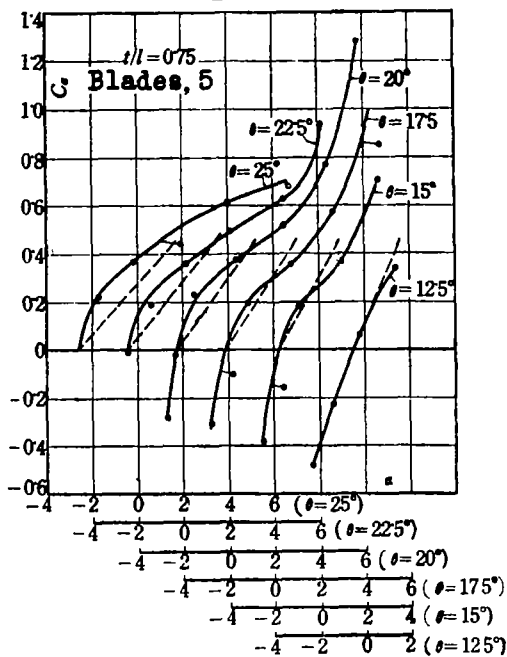
Figure 15.
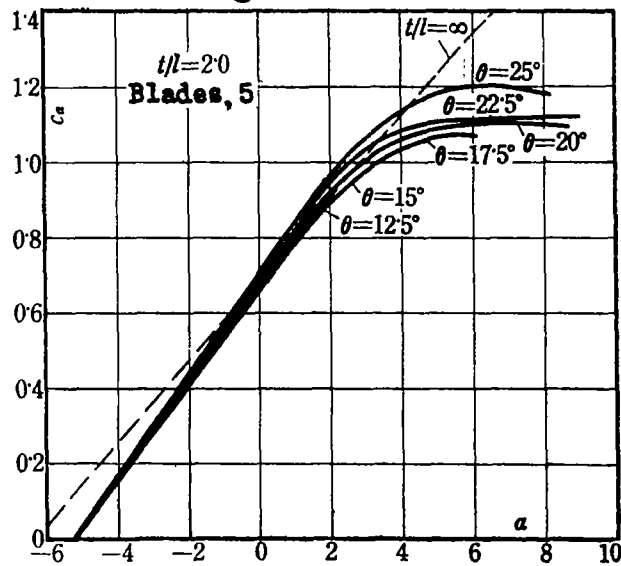
Figure 16.
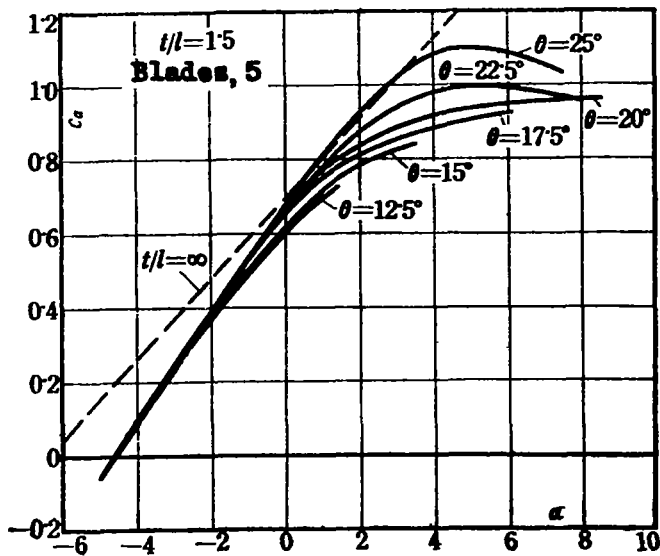
Figure 17.
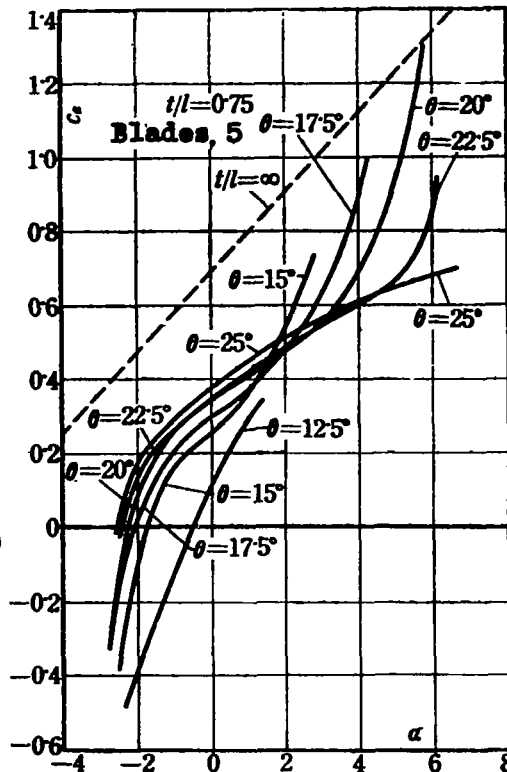
Figure 19.
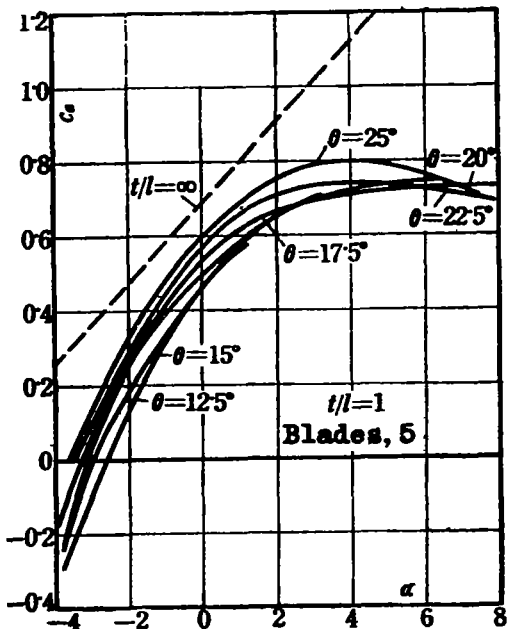
Figure 18.
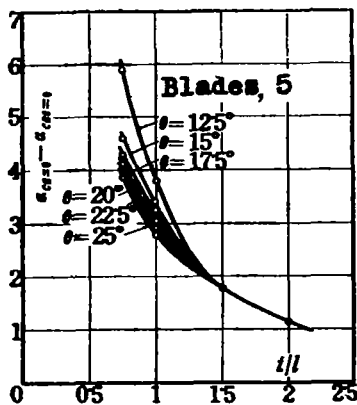
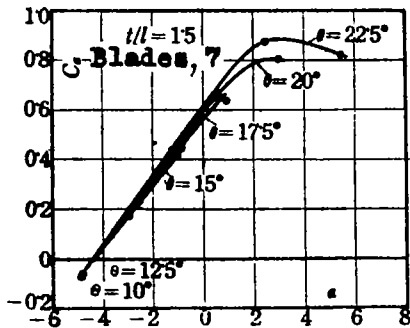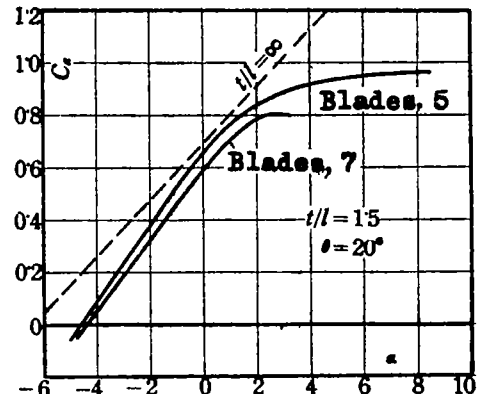

Figure 20.

Figure 21.
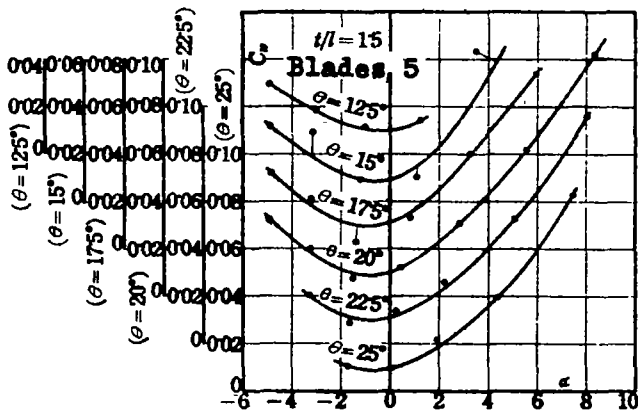
Figure 22.
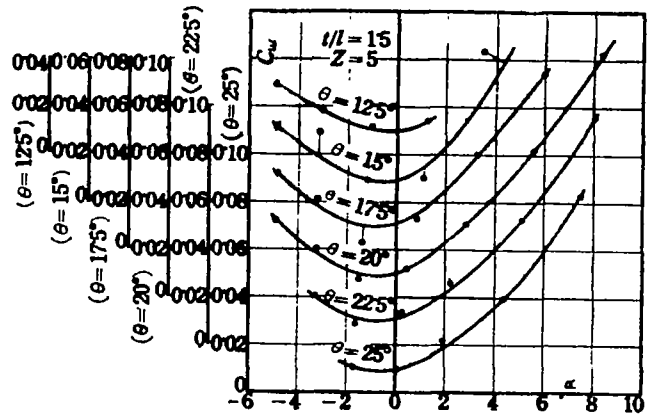
Figure 23.
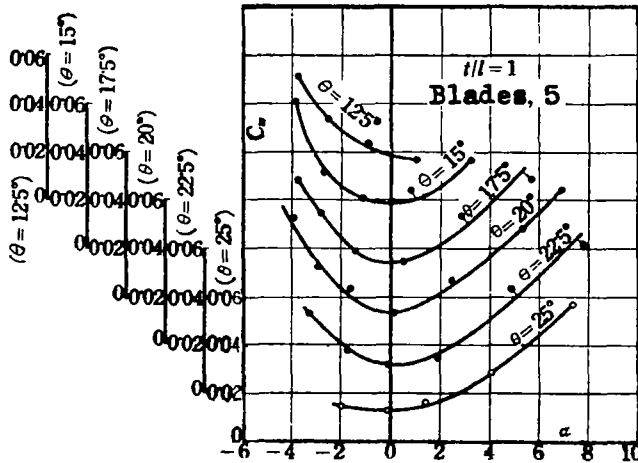
Figure 24.
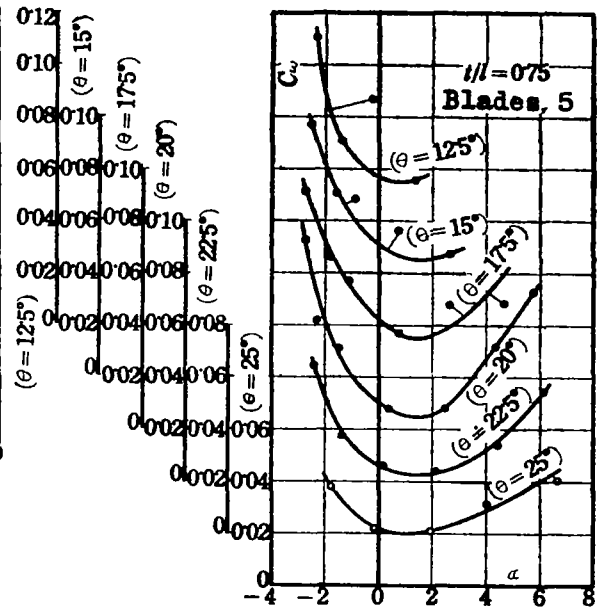
Figure 25.
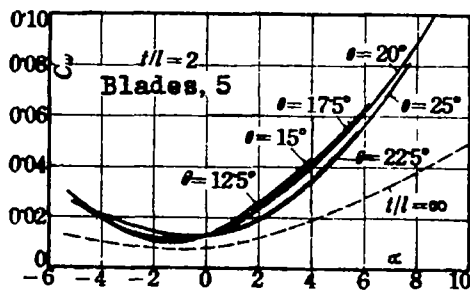
Figure 26.
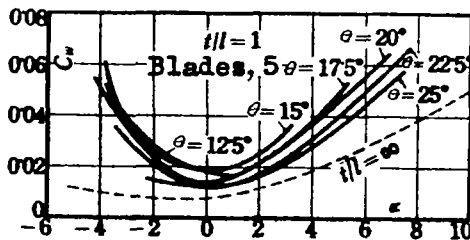
Figure 28.
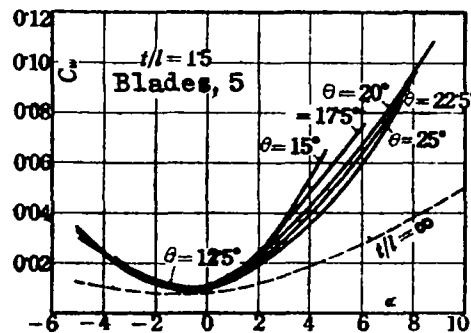
Figure 27.
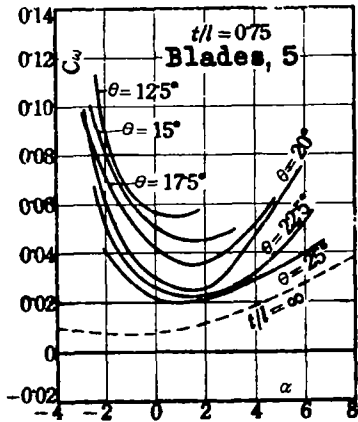
Figure 29.
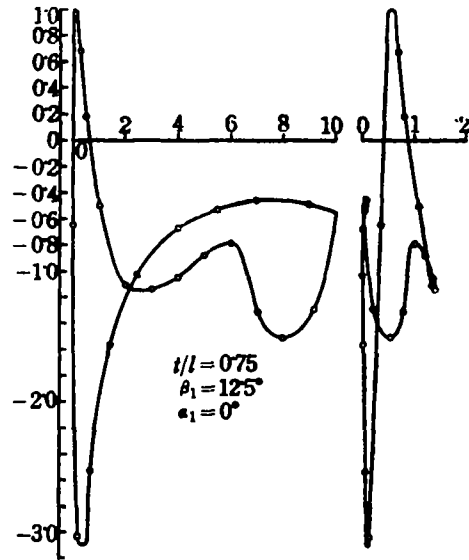
Figure 30.
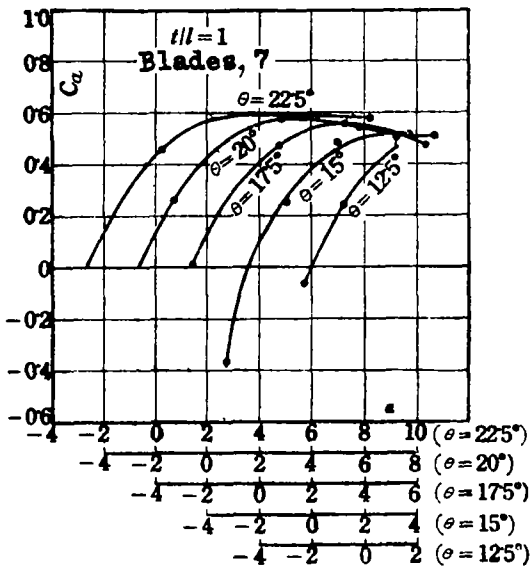
Figure 31.
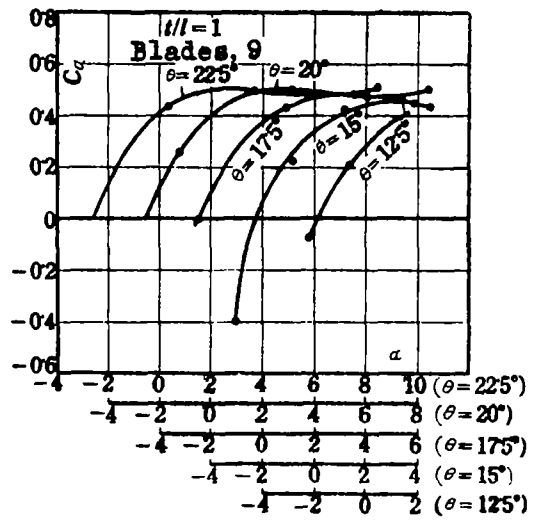
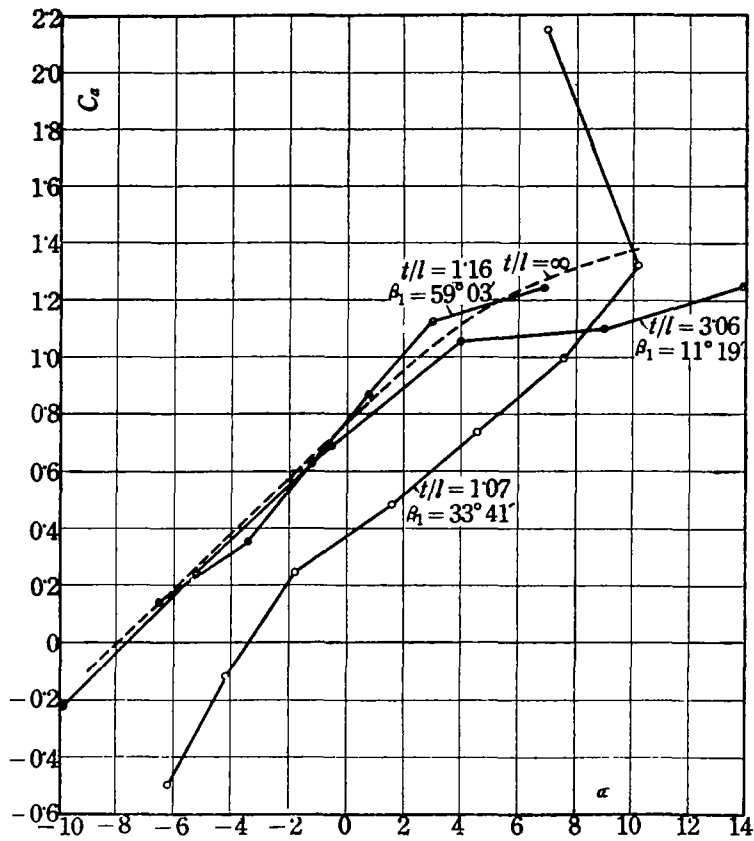

Figure 32.
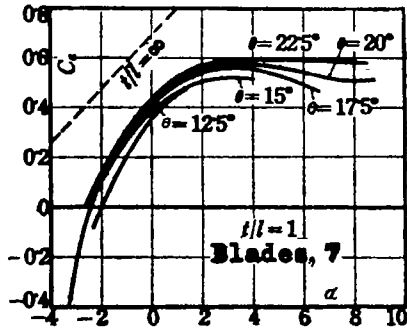
Figure 33.
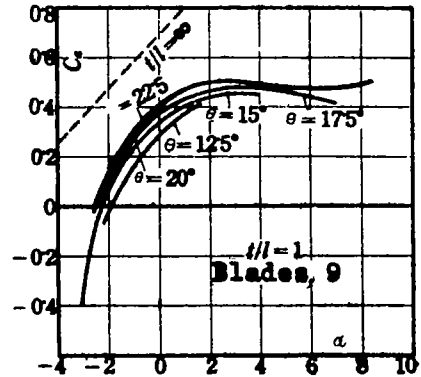
Figure 34.
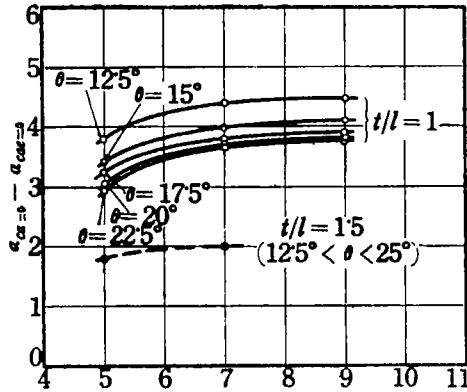
Figure 35.
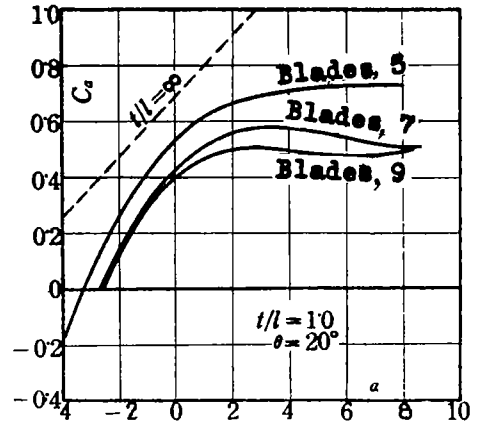
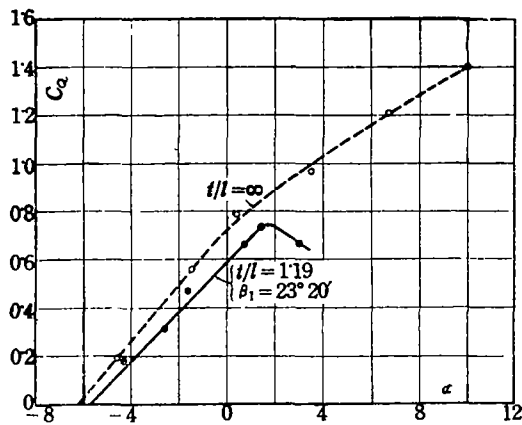Figure 36.

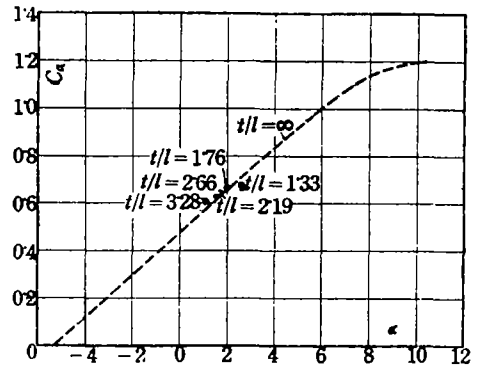Figure 37.

Figure 38.

Figure 39.- Results of Christiani.

Figure 40.

Figure 41.